

# Correcting Motion Artifacts in Magnetic Resonance Images

J.R. Maclaren<sup>1</sup>, P.J. Bones<sup>1</sup>, R.P. Millane<sup>1</sup>, and R. Watts<sup>2</sup>

<sup>1</sup>University of Canterbury, Department of Electrical and Computer Engineering.

<sup>2</sup>University of Canterbury, Department of Physics and Astronomy.

Email: p.bones@elec.canterbury.ac.nz

## Abstract

Motion of the patient during magnetic resonance imaging (MRI) introduces artifacts that can severely degrade the images. A method is proposed to correct for artifacts caused by translational motion, using only information contained in the MRI data. Initial simulation results show the algorithm to be effective in the presence of realistic noise levels. The method is suitable for routine clinical use and could also be applied to MRI diffusion imaging.

**Keywords:** medical imaging, magnetic resonance, MRI, motion artifacts

## 1 Introduction

Magnetic resonance imaging (MRI) is a non-invasive technique routinely used to produce high-quality images of the body's internal tissues. MRI gives excellent discrimination between soft-tissue types for anatomical studies and offers the potential to perform *in vivo* physiological studies.

One disadvantage of MRI in comparison with other scanning modalities, e.g. X-ray CT, is the relatively long data acquisition time required. A typical MRI examination may take anywhere from 20 to 60 minutes (1 - 10 minutes per sequence), so many patients have difficulty remaining still for the required time. If the patient moves during scanning, the image quality is degraded by the appearance of motion artifacts. Common motion artifacts include image blurring and ghosting [1]. This is a particular problem when young children are being imaged and also for claustrophobic patients and patients suffering from illnesses such as Parkinson's disease. Figure 1 shows two images containing motion artifacts. Both are axial slices from a two-month old child. The left image shows severe motion artifacts while the right image is less badly corrupted.

A number of techniques are employed to help ameliorate the problems caused by patient motion. One approach is to prevent the motion occurring by sedation or through the use of physical restraints. While an option for clinical use, sedation is unacceptable for research purposes due to the risk involved. For example, it has been shown that sedation of children for MRI and CT is associated with the risk of hypoxemia [2]. Also,

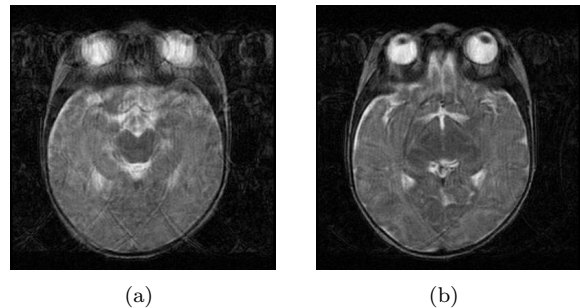


Figure 1: Axial images of the head of a two month-old child showing (a) severe, (b) mild motion artifacts (Lianne Woodward, Canterbury Child Development Research Group, University of Canterbury).

monitoring sedated patients adds an unwanted complication to the scan. Physically restraining patients is only partially effective (even small movements can cause motion artifacts) and may be unpleasant, particularly for those feeling claustrophobic inside the MRI unit.

A second approach is to monitor motion using an external mechanism and use this information to modify the MRI data collected simultaneously. Little work has been done in this area although ultrasound has been used to track motion in conjunction with MRI [3]. One obvious disadvantage is the extra hardware required and the resulting complexity and expense. Systems to monitor respiratory and cardiac motion are common but are not applicable to the problem of bulk motion considered here.

A third and final class of methods to reduce artifacts involve altering the imaging method itself. Such methods include the use of navigator echoes. These attempt to detect translational motion through modified sampling strategies. In the simplest implementation of this technique, an extra line of data is repeatedly sampled. This can then be used to determine motion and corrupted data can be discarded (a disadvantage, as not all data is utilised). Modified versions of navigator echo techniques exist [4, 5], but they all fail to make use of all the collected data for motion correction purposes, reducing scan efficiency.

Perhaps the most promising technique currently available is PROPELLER (Periodically Rotated Overlapping Parallel Lines with Enhanced Reconstruction) MRI [6]. While PROPELLER MRI has been shown to be effective in reducing motion artifacts in simulations [7] and clinical trials [8], it is not yet widely used. This is perhaps because, in common with X-ray CT, a high density of measurements are obtained near the origin of spatial frequency space, while very sparse data is obtained at higher spatial frequencies.

The technique proposed in this paper shares some similarities with navigator echo methods and PROPELLER MRI in that it does not require extra hardware. However the data acquisition and image correction methods differ substantially from existing techniques and thereby offer significant advantages.

## 2 Method

The proposed approach consists of three steps: data acquisition, motion detection and image reconstruction.

### 2.1 Data Acquisition

Data collected during an MRI scan corresponds to samples of the two-dimensional Fourier transform of the image. The domain for this data set is commonly referred to as ‘k-space’ [9]. It can take several minutes of scan time to fully sample k-space (this is why MRI is easily affected by motion) and allow an image to be reconstructed. There are a number of different ways to perform the sampling. These are referred to as ‘k-space trajectories’.

Figure 2 shows the k-space trajectory developed here. K-space is filled using interleaved horizontal and vertical strips. These fill k-space from the origin outwards. Data points within each strip have been raster-scanned using a similar system to other k-space sampling techniques [6]. In this example, the number of strips ( $N$ ) is 16. Note that

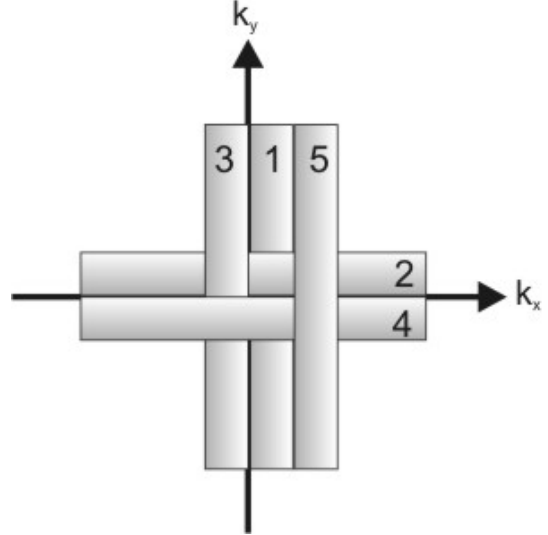


Figure 2: The k-space trajectory used for  $N = 16$ . The first 5 strips are shown; their numbers indicate the order of acquisition.

data is not discarded in the overlapping sections, but is used for both signal averaging and motion detection as described below.

It is assumed that the motion occurring during the acquisition of an individual strip is negligible. For this assumption to be reasonable,  $N$  must be large enough to ensure the acquisition time for each strip is small.

### 2.2 Motion Detection

Each point in k-space is sampled twice: once as part of a vertical strip and once as part of a horizontal strip. If the object is unchanged, both samples will be identical; if the object has been translated by an amount  $(\Delta x, \Delta y)$ , the phase of the second sample will differ from the phase of the first sample by an amount proportional to  $(\Delta x, \Delta y)$  and dependent on the location in k-space,  $(k_x, k_y)$ . Thus the phase difference between matching points within one overlapping region is given by

$$\Delta\phi = 2\pi(k_x\Delta x + k_y\Delta y) \quad (1)$$

This result can be derived from the Fourier shift theorem. In the presence of measurement errors (and other noise inherent in the MRI system), Eq. (1) is only approximate.

Each overlapping region involves a different pairing of strips. For example, the region immediately to the right and above the k-space origin involves strips 1 and 2 (see Figure 2). Assigning subscripts  $m$  and  $n$  according to the strips’ indices, then,

$$\Delta\phi_{mn} = 2\pi(k_x\Delta x_{mn} + k_y\Delta y_{mn}), \quad (2)$$

$m, n \in 1, 2, \dots, N$  for  $m$  odd,  $n$  even,

where  $N$  is the (even) number of strips. As there are  $N/2$  horizontal strips and  $N/2$  vertical strips, there are  $(N/2)^2$  equations of the form (2). Although there are  $N$  strips, the position of the object at the time strip 1 is measured is taken as the reference position so it is already known. Thus there are  $N - 1$  pairs of unknowns: the  $N - 1$  shifts of the object in image-space between the sampling of each strip.

While Eqs. (1) and (2) are in principle correct, phase can only be measured modulo- $2\pi$ . Therefore the measured phase difference values must be unwrapped in order to be used in Eq. (2). To avoid this problem we use a technique known as phase correlation [10, 11].

The shift theorem for the Fourier transform relates a translational shift in the spatial domain to a linear phase in the Fourier domain (k-space). This relationship can be inverted to estimate  $(\Delta x_{mn}, \Delta y_{mn})$  from the overlap between strips  $m$  and  $n$ , without the need for phase unwrapping. In brief the algorithm is:

1. Compute the phase difference  $(\Delta\phi_{mn})$  for each data point in the overlapping section of strips  $m$  and  $n$ .
2. Shift all phase values so that the central data point has a value of 0 and  $\Delta\phi_{mn}$  is now measured with respect to a new origin.
3. Inverse discrete Fourier transform the phase data to generate an image-space function,  $g(x, y)$ .
4. Find the location of the maximum of  $g(x, y)$ . The scaled coordinates at this location provide an estimate of  $(\Delta x_{mn}, \Delta y_{mn})$ , the shift of the object in image space between the sample times of the two strips.
5. In order to obtain sub-pixel accuracy, steps (3) and (4) are repeated. This time the IDFT in (3) is only computed for values at and around the peak found in (4) and with a 100-fold increase in resolution.

The result of this calculation is information relating the relative displacement of the object between each overlapping strip, i.e. all values of  $(\Delta x_{mn}, \Delta y_{mn})$  are now known. The next step is to estimate absolute displacement values from the relative displacements.

For the example shown in Figure 2, the 8 by 8 grid of strips result in 64 overlapping sections and so 64 equations using this information can be written. Each equation gives the change in position of the object between the sampling of the two overlapping strips in question. As there are only 15 pairs of unknowns in this case (the position of the image during sampling of the first strip is defined as the reference) the resulting system of equations is over-determined. Solving in a least squares sense (using MATLAB's *lsqov* function) results in an estimate of the shift that has taken place in image-space between the sampling of each strip (with respect to the reference strip).

### 2.3 Image Reconstruction

The motion detection algorithm gives the shifts in image-space that occurred between the sampling of the first strip and each subsequent strip. Given this, the phase in each k-space strip can be adjusted to correct for the known motion. This is equivalent to translating each strip of data in image space back to the reference position. The required adjustment to the phase can be easily calculated using Eq. (2). Note that this is simply working backwards: initially the displacement was estimated from the phase shift; now the phase shift is calculated from the displacement.

Data is stored in two arrays: one containing vertical strips and one containing strips taken horizontally. Two corresponding 'phase correction' matrices are created containing the necessary phase shifts for each strip. These phase shifts are then applied to the vertically and horizontally collected arrays of data strips. This results in two corrected k-space images, one from each array. The two images are averaged and finally the inverse Fourier transform is applied. This produces a final, motion corrected, image. This procedure is shown in Figure 3.

The advantage of this method is that all the acquired data is used for both motion detection and, in its corrected form, for final image reconstruction.

## 3 Results and Discussion

Initially, the Shepp-Logan head phantom [12] has been utilised for testing purposes. It is widely used in medical imaging and is the sum of ten ellipses of varying size and orientation. It is particularly useful because its Fourier transform can be calculated analytically.

Simulations conducted to test the effectiveness of the algorithm are shown in Figures 4 and 5. In

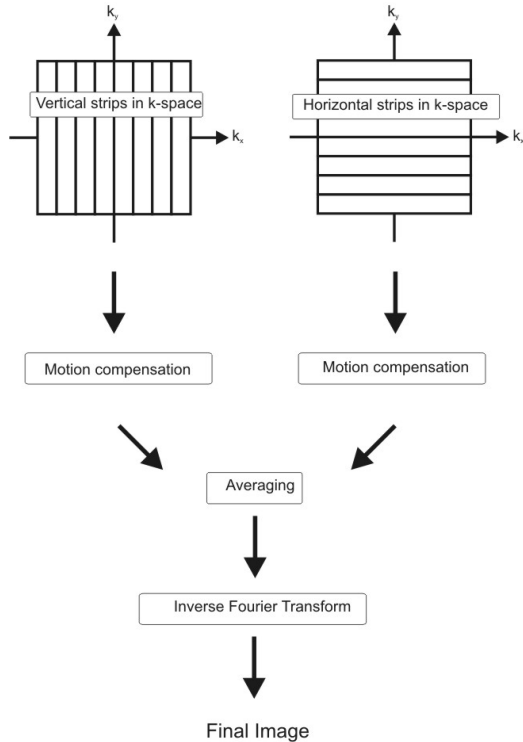


Figure 3: Reconstruction procedure.

all cases,  $N$ , the number of strips used for the simulation, is 16. Figure 4 shows the effect of a linear shift of the object during imaging of 30 pixels in the positive  $x$ -direction and 15 pixels in the positive  $y$ -direction. In comparison, the image resolution is  $256 \times 256$  pixels. For noise-free conditions the results shown in (a), (b) and (c) are obtained. These show the original Shepp-Logan phantom and the uncorrected and corrected images respectively. Using a signal-to-noise ratio (SNR) of 20 dB produces the images shown in (d), (e) and (f). SNR is calculated on the basis of signal ‘energy’, averaged over the entire field of view. Figure 5 (a), (b) and (c) are the same as Figure 4 (d), (e) and (f) except the simulated motion is a ‘random walk’ rather than a linear shift.

The results shown indicate that the algorithm is effective in the presence of noise. Based on the analysis of existing MRI images, the SNR can be assumed to be 20 dB or better in clinical use (when calculated as described).

The quality of the corrected image is unaffected by the degree of motion occurring during the scan time, provided the phantom remains within the FOV. Thus the difference between the corrected and the uncorrected images becomes greater with increasing amounts of motion.

The key advantage of the technique presented here is its efficiency. The same acquisition time and SNR as a conventional algorithm (sampling twice

then averaging) can be achieved. However, unlike a conventional algorithm, the acquired data can also be used to detect and correct for translational motion occurring in image-space. Thus, motion correction information is gained at no cost in acquisition time. This is what sets the proposed technique apart from others.

Sampling over a Cartesian grid gives the algorithm an additional advantage over PROPELLER MRI and some navigator techniques. Data is already in a form suitable for application of the inverse Fourier transform without having to resort to the use of a gridding algorithm.

Currently, no assumptions are made about the nature of the translational motion as a function of time. By incorporating prior knowledge of the maximum possible values of velocity or acceleration, results in the presence of noise should be improved further. A key development will be modification of the existing algorithm to compensate for motion artifacts caused by rotation. This will involve using the magnitude of the  $k$ -space data (rotated with respect to a rotation in image-space).

## 4 Conclusion

The newly proposed algorithm uses an interleaved acquisition of horizontal and vertical strips to fill  $k$ -space. This has several advantages over existing methods. All collected data is used for both motion correction and image reconstruction resulting in a more efficient (and hence more effective) algorithm. Secondly, all data is collected on a Cartesian grid. This means there is no need for gridding of data before applying the Fourier transform.

This technique could be applied in clinical MRI, particularly in cases where motion artifacts are problematic. However, the current algorithm can only detect and compensate for translational, in-plane motion. Work is continuing on extending the described approach to correct for rotation. Clinical trials are planned once this stage is complete.

## References

- [1] Z.-P. Liang and P. C. Lauterbur, *Principles of magnetic resonance imaging : a signal processing perspective*. New York; Bellingham, Wash: IEEE Press; SPIE Optical Engineering Press, 2000.
- [2] S. Malviya, T. Voepel-Lewis, O. P. Eldevik, D. T. Rockwell, J. H. Wong, and A. R. Tait, “Sedation and general anaesthesia in children undergoing MRI and CT: adverse events and

- outcomes,” *Br. J. Anaesth.*, vol. 84, no. 6, pp. 743–748, 2000.
- [3] M. Günther and D. A. Feinberg, “Ultrasound-guided MRI: Preliminary results using a motion phantom,” *Magnetic Resonance in Medicine*, vol. 52, no. 1, pp. 27–32, 2004.
- [4] Y. M. Kadah, A. A. Abaza, A. S. Fahmy, A. B. M. Youssef, K. Heberlein, and X. P. P. Hu, “Floating navigator echo (FNAV) for in-plane 2D translational motion estimation,” *Magnetic Resonance in Medicine*, vol. 51, no. 2, pp. 403–407, 2004.
- [5] A. F. Costa, D. W. Petrie, Y. F. Yen, and M. Drangova, “Using the axis of rotation of polar navigator echoes to rapidly measure 3D rigid-body motion,” *Magnetic Resonance in Medicine*, vol. 53, no. 1, pp. 150–158, 2005.
- [6] J. G. Pipe, “Motion correction with PROPELLER MRI: Application to head motion and free-breathing cardiac imaging,” *Magnetic Resonance in Medicine*, vol. 42, no. 5, pp. 963–969, 1999.
- [7] A. B. Cheryauka, J. N. Lee, A. A. Samsonov, M. Defrise, and G. T. Gullberg, “MRI diffusion tensor reconstruction with PROPELLER data acquisition,” *Magnetic Resonance Imaging*, vol. 22, no. 2, pp. 139–148, 2004.
- [8] K. P. N. Forbes, J. G. Pipe, C. R. Bird, and J. E. Heiserman, “PROPELLER MRI: Clinical testing of a novel technique for quantification and compensation of head motion,” *Journal of Magnetic Resonance Imaging*, vol. 14, no. 3, pp. 215–222, 2001.
- [9] C. B. Paschal and H. D. Morris, “K-space in the clinic,” *Journal of Magnetic Resonance Imaging*, vol. 19, no. 2, pp. 145–159, 2004.
- [10] C. D. Kuglin and D. C. Hines, “The phase correlation image alignment method,” *Proc. IEEE Int. Conf. on Cybernetics and Society*, pp. 163–165, 1975.
- [11] Q. X. Wu, P. J. Bones, and R. H. T. Bates, “Translational motion compensation for coronary angiogram sequences,” *IEEE Transactions on Medical Imaging*, vol. 8, no. 3, pp. 276–282, 1989.
- [12] L. A. Shepp and B. F. Logan, “Fourier reconstruction of a head section,” *IEEE Transactions on Nuclear Science*, vol. NS21, no. 3, pp. 21–43, 1974.

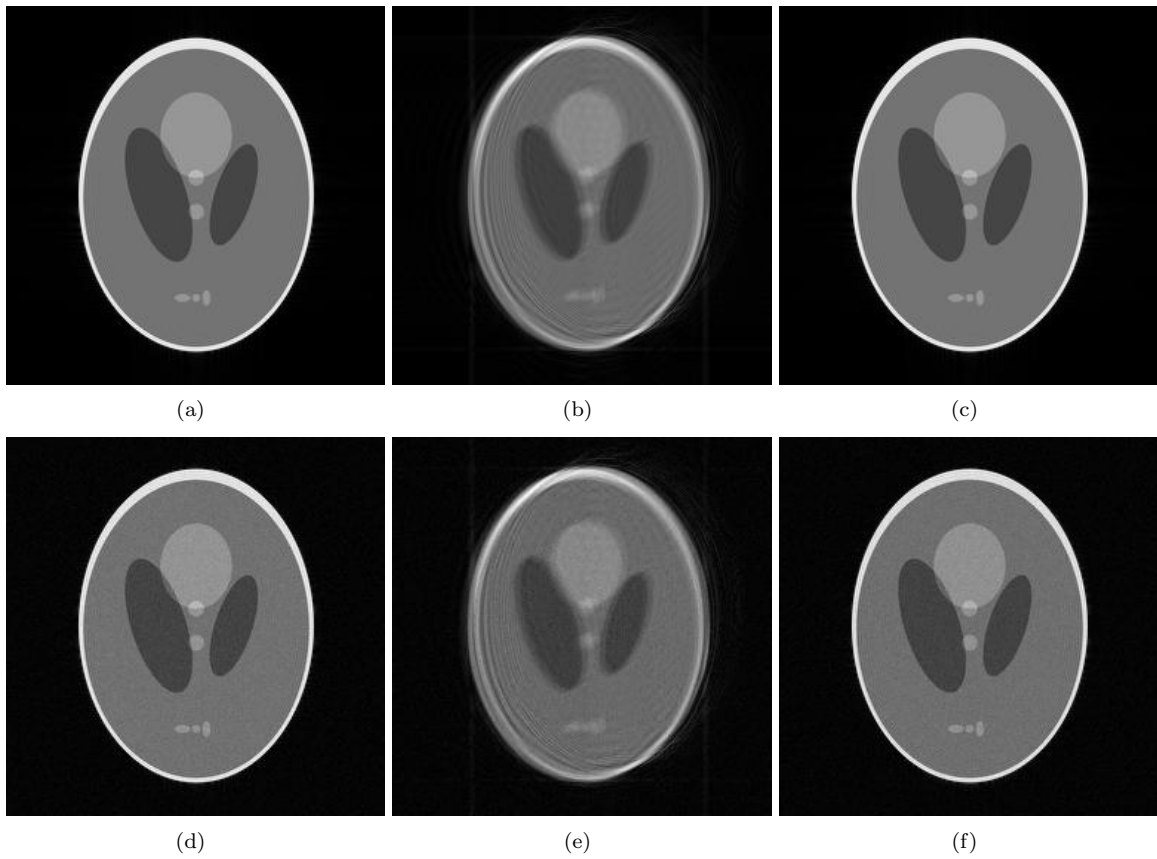


Figure 4: Simulation results for a linear shift: image (a) shows the original Shepp-Logan head phantom; images (b) and (c) show uncorrected and corrected images resulting from data acquisition during phantom movement of 30 pixels horizontally and 15 pixels vertically; images (d), (e) and (f) show the effect of adding noise (20 dB SNR).

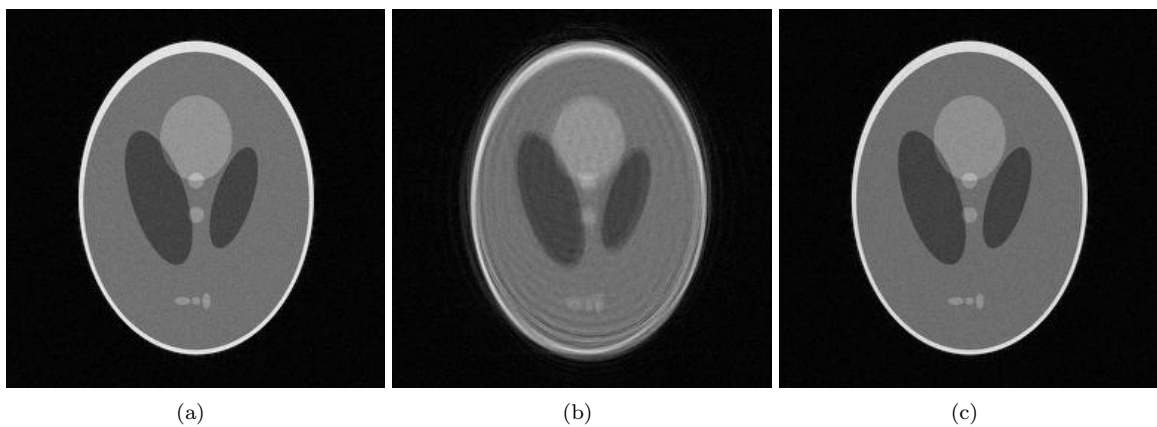


Figure 5: Simulation results for a 'random walk': image (a) shows the original Shepp-Logan head phantom; images (b) and (c) show uncorrected and corrected images resulting from data acquisition during the period of motion. Again, a 20 dB SNR is used.